ACCELERATORS FOR MEDICINE
AND OTHER APPLICATIONS

Thin-Film Detector for Ion Registration in Accelerator Mass Spectrometers

V. V. Parkhomchuk, A. V. Petrozhitskii, and S. A. Rastigeev

Budker Institute of Nuclear Physics, Siberian Branch, Russian Academy of Sciences, Novosibirsk, Russia

Abstract—This paper describes the construction and results of tests of thin-film ion detectors for an acceleration mass spectrometer (AMS). The spectrometer has been developed and constructed in the Budker Institute of Nuclear Physics (BINP) for the Siberian Branch of the Russian Academy of Sciences. A telescope made from several consecutively passed counters provides a low background.

INTRODUCTION

When secondary electrons are knocked out of the film and registered using a microchannel plate (MCP), it is quite easy to obtain a time resolution of $\tau = 0.5$ ns. When the noise loading of one MCP is $f_0 = 100$ Hz, the rate of random coincidence of three series counters is $f_{noise} = f_0^3 \tau^2 = 2.5 \times 10^{-13}$ Hz. When registering a ^{14}C isotope, which is below 10^{-12} of the main isotope ^{12}C, the background created by the charge exchange processes should be decreased at least to the level of 10^{-14}–10^{-15}. When the current of ^{12}C^{+3} is 1 μA at the outlet of the acceleration mass spectrometer (AMS), the flux of ^{14}C is 2 Hz from the contemporary sample and 5×10^{-3} Hz from the sample with a radiation age 50000 years. Obviously, the telescope of three detectors reliably suppresses the random coincidence background. The use of thin films allows the low-energy particles (^{14}C^{+3} carbon, 4 MeV) to pass several consecutive detectors.

Scattering and Deceleration in Films

The detectors involved film targets made of nitrocellulose produced at our institute. The films were produced using a well-known technology [1]: nitrocellulose solution in isoamyl acetate was spread over water surface followed by its precipitation onto the ring with a supporting net. If the average drop weight was 25 ± 2 mg, the concentration nitrocellulose solution was 6 wt % and the average stain diameter was 14 cm; the film thickness was 10 μg/cm^2. The weight of the drop of the solution was controlled by the inner diameter of the pipette tip. For conductivity purposes, a thin layer of aluminum was sprayed onto the surface. The thickness of the layer was controlled by the absorption of infrared light. For a wavelength of 589 nm, the absorption factor was $\alpha = 10^6$ 1/cm;

therefore, 10% absorption corresponded to a 1-nm-thick aluminum layer, or 0.27 μg/cm^2.

To estimate the deceleration of ions in the target, we used table data of SRIM [2]. For the deceleration of the 4-MeV carbon ions in 10-μg/cm^2-thick carbon, the energy losses were 73.8 keV.

The fluctuations of energy losses in the target were estimated as 10 keV. Therefore, the contribution of the energy dispersion of the ions after the target passes into the time resolution was about 0.04 ns.

The multiple-scattering angle of carbon ion in a 10-μg/cm^2-thick carbon target was estimated as 3.6 mrad. The simulation of the scattering in SRIM yielded a value of 3.4 mrad. Therefore, the scattering in the film was rather low.

In our first experiments, we used detectors based on an electrostatic mirror [3]. In this construction four nets placed along the track of the ion beam provided the isochronous transport of secondary electrons from the target into the MCP. In order to reduce the number of nets, we constructed a detector involving a drift of the secondary electrons in crossed magnetic and electric fields (cycloidal detector) [4]. As a result, we managed to increase the transparency of the detector twice in comparison with the construction of the electrostatic mirror.

One important feature of the developed detector is the two-sided collection of the secondary emission from the film onto the MCP assemblies. It increased the efficiency of ion registration when compared to one-sided collection in the construction of the electrostatic mirror.

DETECTOR CONSTRUCTION

The final detector of the AMS was a time-of-flight telescope consisting of three time-of-flight intervals (Fig. 1) which were formed by electrostatic, cycloidal, electrostatic, and edge detectors, respectively. The last
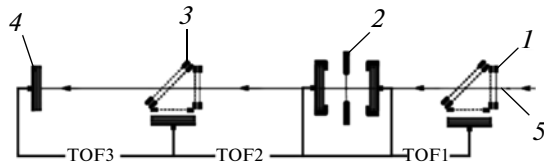
Fig. 1. Scheme of the final detector of the AMS. (*1*) First electrostatic mirror, (*2*) cycloidal detector (sectional view from the side), (*3*) second electrostatic mirror, (*4*) edge detector, and (*5*) direction of ion movement.
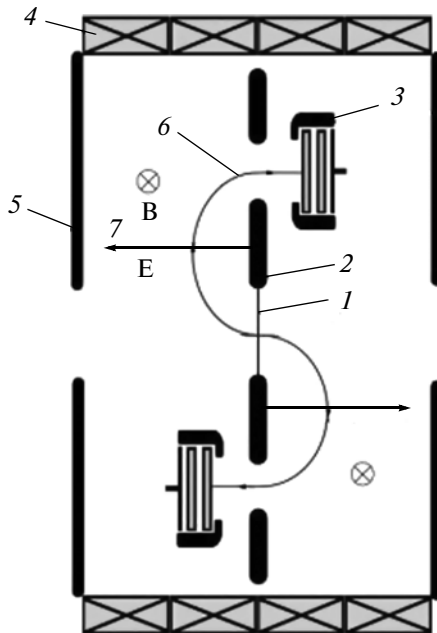

Fig. 2. Scheme of the field and trajectories in cycloidal detector. (*1*) Target, (*2*) central electrode, (*3*) MCP assemblies, (*4*) permanent magnets assemblies, (*5*) edge electrodes, (*6*) trajectory of secondary electrons, and (*7*) longitudinal electric and transverse magnetic field.

Fig. 3. The view of the detector from inside. (*1*) Detector flange, (*2*) hole for the secondary emission, (*3*) magnetic pole, (*4*) assemblies of permanent magnets, (*5*) isolator, (*6*) central electrode, (*7*) target, (*8*) edge lug, (*9*) CP-50 connector, (*10*) edge electrode, and (*11*) MCP assembly.

detector was an assembly of two MCPs subjected directly to the beam; it is not currently in use. The distance between the targets was 24 cm and 19 cm for the two flight intervals, respectively,

Construction of Cycloidal Detector

The cycloidal detector performed the two-sided collection of the secondary emission from the film onto separate MCPs using electron drift in crossed electric and magnetic fields (the trajectory was cycloid). The isochronism of the electron transport from different points of the target was provided by the uniformity of the fields (Fig. 2).

The uniform transverse magnetic field in the region of electron movement was created by four assemblies of permanent NdFeB magnets placed between the magnetic poles. This construction did not require an extern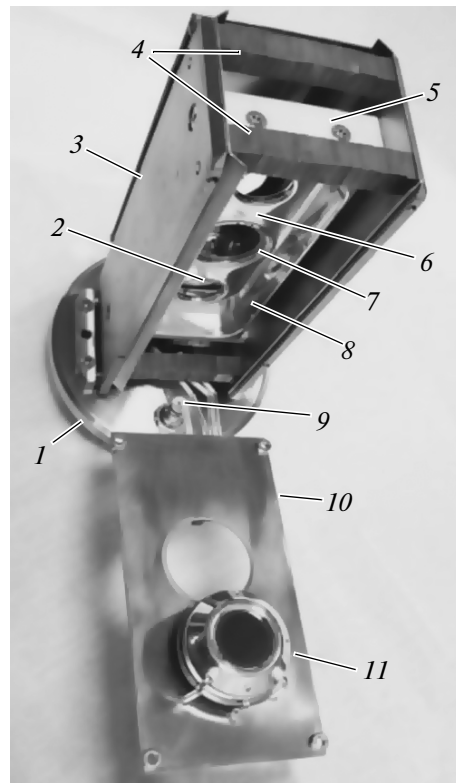al current source, so it could be placed entirely into a vacuum. The magnetic poles had lugs in order to compensate the edge effects. The value of the magnetic fields was 145 Gs. The magnetic system of the detector was under zero potential and was the load-bearing part of the construction.

Due to the small sizes of the area of the uniform magnetic field, we decided to substitute distributing electrodes with voluminous edge lugs on the central electrode in order to simplify the construction. The electrode was milled from dural and insulated from the magnetic system. The voltage on this electrode was −7 kV, corresponding to the electric field 2.2 kV/cm in the region of electron movement.

In order to lock the secondary emission on the surface of the MCP, we used the accelerating potential of the electrode. For this purpose the assemblies were isolated from the central electrode and placed on the opposite side towards the trajectory of the secondary electrons (Fig. 2). Though holes were made in the central electrode for this purpose. Each assembly consisted of two MCPs separated with a 50-μm-thick copper packing. The assemblies were attached to the edge electrodes to the collectors using the isolators (Fig. 3). The front surface of the first MCP was electrically connected to the assembly corpus, where the voltage was −2.6 kV.
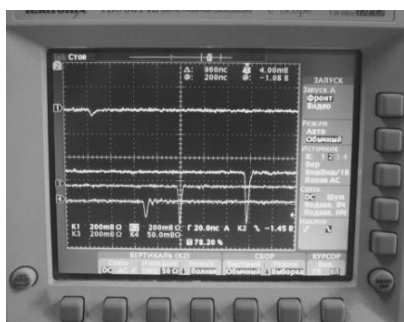
Fig. 4. Oscillograph chart of the signals. (*1*) Signal from the first electrostatic sensor, (*2, 3*) signals from the cycloidal sensors, and (*4*) signal from the second electrostatic mirror.
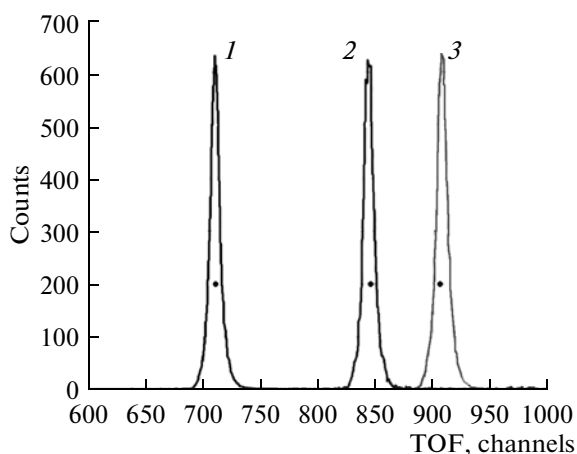

Fig. 5. Spectrum of the time of flight between the first and the third detectors. (*1*) TOF spectrum of ^{10}B, (*2*) TOF spectrum of ^{14}C, and (*3*) TOF spectrum of ^{16}O.

Fig. 6. Two-dimensional time-of-flight spectrum.

The voltage was applied onto the detector from two high-voltage sources. The central electrode and two MCP assemblies were powered by separate dividers. The voltage input into vacuum was made through 32-pin connector. The signals from the collector of the MCP were output through CP-50 connectors.

The target aperture of the detector was 28 mm. For the production of the supporting net, we used fibers of gold-plated tungsten (30 μm in diameter) deposited with a step of 1 mm onto the stainless steel ring. It corresponded to a 97% target transparency. Nets (30 μm, 3-mm step) were attached onto the edge electrodes though the inlet aperture in order to prevent the collapses of the electric field. The resultant transparency of cycloidal detector was 95%.

Construction of the Electrostatic Mirror

The first and third detectors of the time-of-flight telescope were made using the traditional scheme of angled electrostatic reflector. The isochronism of the transport of the secondary emission from the target to the MCP was achieved by the geometrical equality of the paths. The one-sided collectio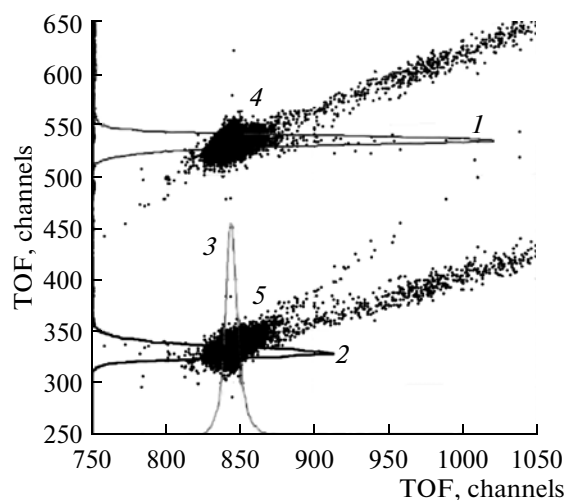n of the secondary emission was organized in the detector. The secondary electrons from the target declined for 90° and were enhanced in the tandem of two MCPs. The aperture of the detector was 20 mm; the target was manufactured using the previously described technology. The voltage between the target and the accelerating net was 1.5 kV, and the split was 5 mm. The front and the bottom side of the prism were 45 mm in size. The supporting and accelerating nets were welded on from the fibers of gold-plated tungsten with a 30 mm diameter with a 1-mm step; the step of the nets of the electrostatic mirror was 1.5 mm. The voltage between them was 3 kV and the split was 7 mm. The resultant transparency of the detector was 90%.

MEASUREMENT OF DETECTOR PARAMETERS

Since the main application of the developed AMS was radiocarbon dating, the final detector should have separated the weights which were close to 14 amu. Figure 4 shows the oscillograph chart of the signals from four sensors of the final detector after of the flight of ^{13}C ion.

At the moment, the voltage at the AMS terminal is 1 MV. The charge state of the ions after the charge exchange was 3+. The energy of negative ions at the output of the source was 25 kV. Therefore, the energy of the ions at the input into the time-of-flight detector was 4.025 MeV. Figure 5 shows the spectrum of the times of flight between the first and third detectors (TOF 1−3), when the outlet magnet of the AMS was adjusted for different isotopes. The AMS was adjusted for the transmittance of 14-amu weight.

In order to examine the stability of the AMS operation, we carried out a series of measurements of 12 samples of carbon fibers which were tested as a fine reproducible standard of a contemporary electrode. Figure 6 shows the two-dimensional spectra of the

times of flight of ^{14}C ions in these two intervals. The horizontal axis shows the time of flight (channels; 0.07 ns/channel) from the first to the third counter; the upper half on the Y axis stands for the time of flight in the first interval and the lower half stands for the time of flight in the second one. The histograms of the corresponding times of flight are shown with solid lines. The 'tails' of the scattered ions are clearly seen on the first film and less obvious on the second one. The time resolution was 0.65 ns by channel 1−2 and 0.45 ns by channel 1−3.

At the moment, the efficiency of the ion registration with a cycloidal detector with a two-sided collection of the knocked-out electrodes is close to 100%; the efficiency of the detector with an electrostatic mirror is about 80%. When a beam of ^{13}C ions with a 10 nA current gets onto the films, a rapid partial destruction of the films occurs, which leads to the reduction of the counting efficiency. The destruction may be associated with the low conductivity of the films and requires an increase in the sprayed-on layer. It should be noted that the detectors can operate in a range of counting rates of up to 50 kHz.

CONCLUSIONS

This study resulted in the creation of a prototype of a time-of-flight detector. Currently the time resolution of 0.45 ns is sufficient. On the whole, the studies show that the developed system is functional, but the characteristics of the created detector should be further improved. It is necessary to use thinner carbon targets, which can improve the time resolution and increase the efficiency of the registration.

REFERENCES

1. E. Angerer, H. Ebert, and W. Summer, *Physical Laboratory Handbook* (Pitman Publ., London, 1966; Fizmatgiz, Moscow, 1962), rus. p. 128.
2. J. F. Ziegler, Nucl. Instrum. Methods Phys. Res. B **136**, 141 (1998).
3. N. I. Alinovskii et al., "A Time-of-Flight Detector of Low-Energy Ions for an Accelerating Mass-Spectrometer," Instrum. Exp. Tech. **52**, 234 (2009).
4. J. D. Bowman and R. H. Heffner, "A Novel Zero Time Detector for Heavy Ion Spectroscopy," Nucl. Instrum. Methods Phys. Res. **148**, 503−509 (1978).